Colloid Polym Sci 279:571–578 (2001)

ORIGINAL CONTRIBUTION

T. Okubo
H. Ishiki

Rigidity of colloidal alloys as studied by reflection spectroscopy in sedimentation equilibrium

Received: 14 June 2000
Accepted: 3 November 2000

T. Okubo (✉) · H. Ishiki
Department of Applied Chemistry
Faculty of Engineering, Gifu University
Gifu 501-1193, Japan
e-mail: okubotsu@apchem.gifu-u.ac.jp
Fax: +81-58-2932628

Abstract Rigidities of colloidal alloys of binary mixtures of colloidal silica spheres (CS82; 103 nm in diameter) with larger silica spheres (CS91; 110 nm, CS121; 136 nm and CS161; 184 nm) have been measured by reflection spectroscopy in sedimentation equilibrium. Substitutional-solid-solution-type alloy structures are formed for mixtures of CS82 and CS91 and for CS82 and CS121. A superlattice, probably $MgCu_2$ type, is formed for CS82 and CS161 mixtures. The rigidities of the colloidal crystals of the single component of the spheres increase as the sphere size increases at the same number density of spheres. The rigidities of the colloidal alloys decrease when a comparatively small number of the larger spheres are mixed with the small spheres at the same total sphere number density.

Key words Colloidal alloys · Colloidal silica sphere · Rigidity · Reflection spectroscopy · Superlattice

Introduction

Recently, keen attention has been paid to the colloidal crystals, i.e., crystal-like distribution of colloidal particles in suspensions of aqueous and organic solvents [1–13]. Many researchers have studied interparticle interaction, lattice structure, morphology of single crystals, phase transitions, crystallization kinetics of nucleation and crystal growth, physicochemical properties (rigidity, viscosity, etc.), structural changes induced by external fields such as gravity, centrifugal and electric fields and shearing forces, for example. The colloidal crystal has been studied mainly for two groups: dilute and deionized aqueous suspensions [14–26] and concentrated suspensions in refractive-index-matched organic solvents [27–32]. The former are very convenient models for both the soft and hard sphere systems depending on the ionic concentrations of the suspension, i.e., soft crystals in the exhaustively deionized state and hard crystals in the presence of rather large amounts of sodium chloride, for example. Colloidal crystallization of soft sphere systems takes place for monodispersed colloidal particles in suspension. Many researchers have clarified that the colloidal crystals are formed by Brownian movement of colloidal size of particles resulting in interparticle repulsion by minimizing the dead space which is not occupied by the particles [11, 20, 25]. In other words, each system forms a crystal-like distribution automatically with the help of Brownian movement of each particle in order to maximize the packing density. Thus, colloidal crystallization is one of the typical systems of three-dimensional auto-organization.

When the extra repulsive interaction, like electrostatic repulsion, is effective among colloidal particles in addition to the repulsion forces from their Brownian movement, colloidal crystallization takes place easily even at very low particle concentrations. Most colloidal particles get negative charges on their surfaces in polar solvents like water. The ionic groups leave their counterions and these excess charges accumulate near the surface forming an electrical double layer. The counterions in the diffuse region are distributed according to a balance between the thermal diffusion forces (“repulsive”) and the forces of electrical attraction with colloidal particles. The thickness of the electrical double

layers is estimated approximately by the Debye screening length, D_l, given by Eq. (1). The Debye length corresponds to the distance from the colloidal surface, where the electrostatic potential decreases to 1/2.7 compared to that at the slipping zone.

$$D_1 = (4\pi e^2 n/\varepsilon k_B T)^{-1/2} \quad (1)$$

Here, e is the electronic charge and ε is the dielectric constant of the solvent. n is the concentration of "diffusible" or "free-state" cations and anions in suspension; thus, n is the sum of the concentrations of diffusible counterions (n_c), foreign salt (n_s) and both H^+ and OH^- from the dissociation of water (n_0), $n = n_c + n_s + n_0$. The maximum value of D_l in water is about 1 μm, which is estimated from Eq. (1) by taking $n_0 = 2 \times 10^{-7}$ mol/dm^3 $\times$ $N_A \times 10^{-3}$ cm^{-3}, where N_A is Avogadro's number. It should be noted that the electrical double layers are always formed in solid-in-polar-liquid-type colloidal dispersions.

In the deionized state, the electrical double layer is very thick, and the interparticle repulsive forces prevail to a long distance, as long as micrometers, though the forces come to be very weak. Formation of the crystal-like ordering is explained nicely with the effective soft-sphere model. The effective diameter, d_{eff}, of spheres includes the Debye screening length and is given by the diameter plus twice the Debye length. When d_{eff} is shorter than the observed intersphere distance, D, a gaslike distribution is observed. When d_{eff} is comparable to or a bit shorter than the intersphere distance, the distribution of spheres is usually liquid-like. When the effective diameter is close to or larger than the observed intersphere distance, crystal-like ordering occurs. The effective soft-sphere model has been shown to be good by many researchers from the systematic comparison between d_{eff} and D values [11, 20, 25].

For binary mixtures of monodispersed colloidal spheres, alloy structures have been studied by Hachisu and Yoshimura [33, 34]. The superlattice structures observed hitherto are AlB_2, $NaZn_{13}$, $CaCu_5$, $MgCu_5$ and AB_4 types. These structures have been analyzed successfully based on the effective soft-sphere model. The structure type was determined beautifully by the ratio (γ) of the effective diameters, including the Debye screening length of the constituent spheres [33–35]. This work reports the rigidity of colloidal alloys of colloidal silica spheres in soft-sphere systems.

Experimental

Materials

Colloidal silica spheres of CS82, CS91, CS121 and CS161 were gifts from Catalyst & Chemicals Ind. Co. (Tokyo). The diameter (d_0), the standard deviation (δ) from the mean diameter and the polydispersity index (δ/d_0) of these spheres are compiled in Table 1. The values of d_0 and δ were determined using an electron microscope. The charge density of the spheres was determined for strongly acidic groups by conductometric titration with a Horiba model DS-14 conductivity meter. The sphere samples were carefully purified several times using an ultrafiltration cell (model 202, membrane: Diaflo-XM300, Amicon Co.). Then, the samples were treated on a mixed bed of cation- and anion-exchange resins [Bio-Rad, AG501-X8 (D), 20–50 mesh] for more than 4 years before use, since newly produced silica spheres always released a considerable number of alkali ions from the sphere surfaces for a long time. The water used for the purification and for the suspension preparation was purified using a Milli-Q reagent grade system (Milli-RO5 plus and Milli-Q plus, Millipore Co., Bedford, Mass.).

Reflection spectroscopy

Quartz optical cells (10 mm $\times$ 10 mm $\times$ 70 mm high) with long necks and screw caps were used. A purified suspension of mixed spheres was introduced into the cell with a mixed bed of ion-exchange resins [Bio-Rad, AG501-X8(D)]. Before the start of the measurements of the sedimentation equilibrium, the suspension in the cell was deionized with the resins coexisting for a week by mixing the suspension gently a few times a day. Then, the cells were left to stand for 1–2 months. The reflection spectra at various heights at an incident angle of 90° were recorded on a multichannel photodetector (MCPD-110B, Otsuka Electronics, Hirakata, Osaka) connected to a Y-type optical fiber cable. The instrument was operated by a microcomputer (MC800, Otsuka Electronics).

Results and discussion

Reflection spectroscopy in sedimentation equilibrium

Generally speaking, the shape of a reflection spectrum profile of colloidal crystals is a single peak, a double peak or a single peak with a shoulder [36]. The two-wavelength peaks were always close together, with a difference of only 1.025 in the ratios of their wavelengths. This difference supports the idea that the peak appearing at the longer wavelength is ascribed to the face-centered cubic (fcc) lattice, while the shorter wavelength corresponds to the body-centered cubic (bcc) lattice in the crystal structures. The broken and one-dot broken lines in Fig. 1 show two peaks, with a difference of 1.03 in the ratio of their peak wavelengths in the reflection spectra. Thus, the peaks appearing at the longer and shorter wavelengths are ascribed to the

Table 1 Properties of the colloidal spheres used

Sphere	d (nm)	δ (nm)	δ/d	Charge density (μC/cm^2)
CS82	103	13.2	0.13	0.38
CS91	110	4.5	0.041	0.48
CS121	136	10.9	0.008	0.40
CS161	184	18.6	0.10	0.47

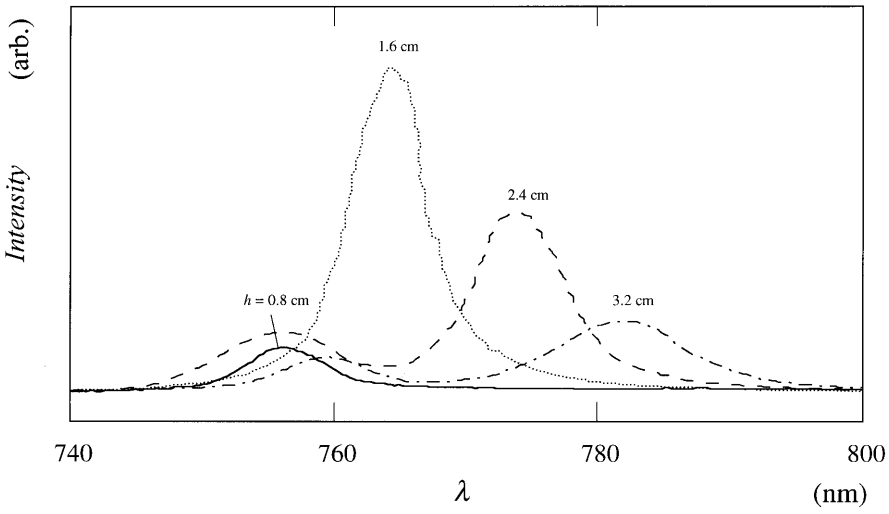

Fig. 1 Height dependence in the reflection spectra of colloidal alloys of CS82 and CS91 mixtures (1:1 in volume fraction) in a sedimentation equilibrium at 25 °C, 45 days after setting the suspension, $\phi_{CS82} = \phi_{CS91} = 0.01$

fcc and bcc lattices, respectively. The intersphere spacing (l) is determined from the peak wavelength [37] and is listed in Tables 2, 3 and 4. For both fcc and bcc lattices the distance at a scattering angle of 180° is given by

$$l = 0.6124(\lambda_p/n_w) \quad (2)$$

where n_w is the refractive index of the sphere suspension (taken as that of water in this work) and λ_p is the peak wavelength.

Typical examples of the reflection spectra of CS82 and CS91, CS82 and CS121 and CS82 and CS161 mixtures at various heights in sedimentation equilibriumare shown in Figs. 1, 2 and 3, respectively. In these figures, the initial concentrations of the four kinds of spheres were 0.01 in volume fraction. All the suspensions displayed brilliant iridescence and the crystallites began to flicker several minutes after the suspensions had been prepared with the mixed beds of cation- and anion-exchange resins in the observation cells. The states of the sedimentation equilibrium achieved 45, 31 and 31 days after the suspensions were set in the observation cells. Clearly, all the alloy crystals were compressed under the gravitational field.

The mean intersphere distance (l_0), when the spheres were distributed homogeneously as the substitutional solid solution (sss) and bcc structures, was calculated using Eq. (3) [35, 38] and is also cited in Tables 2, 3 and 4.

$$l_0 = [(\phi_1/0.68d_{01}^3) + (\phi_2/0.68d_{02}^3)]^{-1/3} \quad , \quad (3)$$

where ϕ_i and d_{0i} denote the volume fraction and diameter of sphere i, respectively. As is clear from Tables 2 and 3, l was very close to l_0 for CS82 and CS91 and for CS82

Table 2 Characteristics of the alloy crystals of CS82 and CS91

ϕ_{CS82}	ϕ_{CS91}	λ_p (nm)	l (nm)	l_0 (nm)	$D_{l,obs}$ (nm)	γ	G (Pa)	g
0.005	0	574.4	529	541	239	(0.99)	17.9	0.045
0.00333	0.00166	613.3	564	537	256	0.99	21.9	0.040
0.0025	0.0025	615.9	567	544	257	0.99	14.9	0.047
0.00166	0.00333	607.1	559	552	253	0.99	11.8	0.0052
0	0.005	617.6	568	582	257	(0.99)	12.8	0.048
0.02	0	744.2	342	343	145	(0.98)	140	0.032
0.0133[a]	0.00667	754.3	346	342	147	0.98	165	0.029
0.0133[b]	0.00667	775.4	356	342	152	0.98	152	0.030
0.01[a]	0.01	754.7	347	344	147	0.98	180	0.027
0.01[b]	0.01	774.0	356	344	151	0.98	154	0.029
0.00667	0.0133	754.0	346	348	146	0.98	147	0.029
0	0.02	777.0	357	367	151	(0.98)	114	0.032
0.05	0	550.0	252	253	100	(0.98)	421	0.029
0.0333	0.0167	564.4	258	251	103	0.98	462	0.027
0.025	0.025	564.6	258	254	103	0.98	450	0.027
0.0167	0.0333	570.1	261	257	104	0.98	315	0.032
0	0.05	581.3	266	270	106	(0.98)	403	0.027

[a] Body-centered-cubic lattice structure
[b] Face-centered-cubic lattice structure

Table 3 Characteristics of the alloy crystals of CS82 and CS121

ϕ_{CS82}	ϕ_{CS121}	λ_p (nm)	l (nm)	l_0(nm)	$D_{l,obs}$ (nm)	γ	G (Pa)	g
0.005	0	574.4	529	541	239	(0.95)	17.9	0.045
0.00333	0.00166	593.5	546	564	246	0.95	20.1	0.039
0.0025	0.0025	626.1	576	597	260	0.95	31.1	0.028
0.00166	0.00333	655.3	603	616	272	0.95	8.3	0.053
0	0.005	659.6	607	715	270	(0.95)	13.9	0.034
0.02	0	744.2	342	343	145	(0.92)	140	0.032
0.0133	0.00667	811.0	373	358	159	0.93	114	0.032
0.01	0.01	828.3	380	372	162	0.93	138	0.028
0.00667	0.0133	871.7	400	391	171	0.93	54.3	0.041
0	0.02	1019.3	468	452	200	(0.94)	87.2	0.027
0.05	0	550.0	252	253	100	(0.90)	421	0.029
0.0333	0.0167	599.3	274	264	110	0.91	240	0.035
0.025	0.025	618.6	283	275	113	0.91	395	0.026
0.0167	0.0333	662.9	303	288	122	0.91	187	0.035
0	0.05	704.2	322	334	127	(0.92)	283	0.024

Table 4 Characteristics of the alloy crystals of CS82 and CS161

ϕ_{CS82}	ϕ_{CS161}	λ_p (nm)	l (nm)	l_0 (nm)	$D_{l,obs}$ (nm)	γ	G (Pa)	g
0.005	0	574.4	529	541	239	(0.88)	17.9	0.045
0.0025	0.0025	867.5	798	638	370	0.91	12.9	0.040
0.0025	0.0025	909.2	837	638	389	0.92	17.1	0.035
0.00166	0.00333	884.4	814	687	376	0.91	6.7	0.050
0.00166	0.00333	904.0	832	687	385	0.92	6.0	0.052
0	0.005	715.5	659	987	283	(0.89)	3.7	0.041
0.02	0	744.2	342	343	145	(0.83)	140	0.032
0.0133	0.00667	718.9	330	373	138	0.82	48.2	0.046
0.01	0.01	773.1	355	397	149	0.83	109	0.028
0.01	0.01	938.9	431	397	187	0.85	74.0	0.034
0.00667	0.0133	796.7	366	435	152	0.83	32.3	0.045
0.00667	0.0133	958.7	440	435	189	0.86	39.9	0.040
0	0.02	631.3	580	612	244	(0.88)	23.2	0.033
0.05	0	550.0	252	253	100	(0.79)	421	0.029
0.0167	0.0333	774.3	354	321	146	0.83	259	0.025
0	0.05	973.3	445	451	177	(0.85)	122	0.023

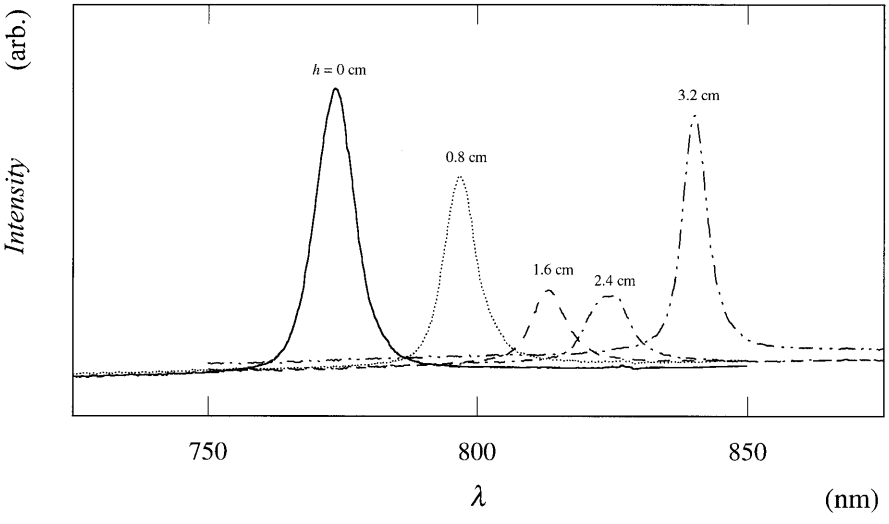

Fig. 2 Height dependence in the reflection spectra of colloidal alloys of CS82 and CS121 mixtures (1:1) in a sedimentation equilibrium at 25 °C, 31 days after setting the suspension, $\phi_{CS82} = \phi_{CS121} = 0.01$

and CS121 mixtures, which strongly suggests that the alloy crystals are formed by the electrostatic intersphere repulsion. The Debye screening length observed, $D_{l,obs}$, was also obtained and is compiled in the tables. The $D_{l,obs}$ values were very close to the calculated values of the Debye length from the number ratio of two spheres

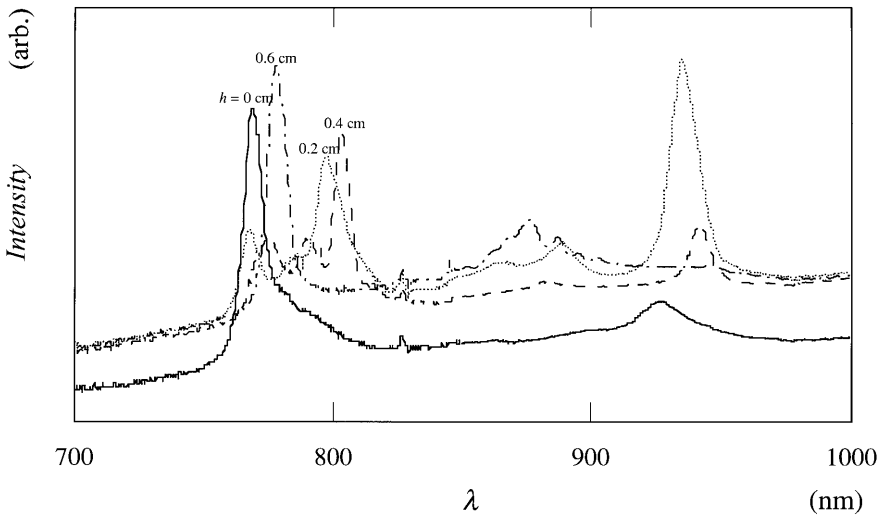

Fig. 3 Height dependence in the reflection spectra of colloidal alloys of CS82 and CS161 mixtures (1:1) in a sedimentation equilibrium at 25 °C, 31 days after setting the suspension, $\phi_{CS82} = \phi_{CS161} = 0.01$

for the binary mixtures using Eq. (2), where the fractions of free-state counterions (β) were assumed to be 0.15, 0.13, 0.12 and 0.07 for CS82, CS91, CS121 and CS161 spheres, respectively. However, the $D_{l,obs}$ values are not cited in Tables 2, 3 and 4 since too many thermodynamic quantities would have to be cited. As shown in Table 4 the l values, which were estimated from the main peaks, especially for the 1:1 CS82 and CS161 mixtures, did not agree with the corresponding l_0 values but were scattered around the calculated values. This is clearly due to the fact that the superlattice structures are formed as described later.

Clearly in the figures, the single peaks appeared for mixtures of CS82 spheres with CS91 or CS121 spheres, whereas several peaks appeared for mixtures of CS82 and CS161 spheres. As is clearly seen in the tables, the ratios (γ) of the effective sizes of two spheres including the Debye screening length were 0.98, 0.93 and 0.83 for CS82 and CS91, CS82 and CS121 and CS82 and CS161 mixtures, respectively, at each sphere concentrations of 0.01 in volume fraction. It is well known that the γ values for the sss-type alloy structures of metals are larger than 0.85 [39]. Thus, the single peaks for the former two kinds of mixtures will be attributed to the sss-type alloy structure. On the other hand, the complex peak profiles having several peaks in the reflection spectra of the CS82 and CS161 mixture shown in Fig. 3 are attributed to the superlattices formed. The exact kind of the superlattices is not clear yet. The observed γ value (0.83) was smaller than 0.85, which is also consistent with the superlattice alloy structure being formed in the mixture [39]. A highly plausible structure would be a $MgCu_2$-type superlattice, γ values of which were reported by Yoshimura and Hachisu [34, 40] to be 0.77–0.84.

It should be mentioned here that the segregation effect, i.e., large spheres are segregated upward and small ones downward in normal gravity, is significant for binary mixtures of colloidal and powder spheres [41–46]. We have studied microscopically the two-dimensional structure of the bottom layers for binary colloidal mixtures of different sizes and densities in sedimentation equilibrium [47]: the segregation effect was substantial. A slight segregation effect has also been observed for the two-dimensional structure of the vertical plane by reflection spectroscopy [35, 37]. In this work, however, the clear-cut segregation effect was not observed, which is mainly due to the fact that the polydispersity indices of the colloidal silica spheres used in this work were comparatively high compared with monodispersed polystyrene spheres, for example.

Rigidity of colloidal alloys

The nearest-neighbor intersphere spacing, l, is given by Eq. (4) [48],

$$l - l_m = (\rho_{eff} g l_m \phi_m / G)(h - h_m) \quad , \tag{4}$$

where l_m and ϕ_m indicate the lattice spacing and the sphere concentration at the midplane, h_m, respectively. ϕ_m is therefore equal to the initial concentration. ρ_{eff} is the effective density given by the specific gravity of the spheres minus that of the solvent, and g is the gravitational constant. G is Young's elastic modulus (rigidity) for the colloidal crystals and was obtained from the slopes of l (or reflection peak wavelength, λ_p, using Eq. 1) versus h shown in Fig. 4, for example. The values of G thus estimated are compiled in Tables 2, 3 and 4.

The logarithms of the G values of the colloidal crystals formed from single components of spheres are shown as a function of the logarithm of the number density (N) of the spheres in Fig. 5. The rigidities of the

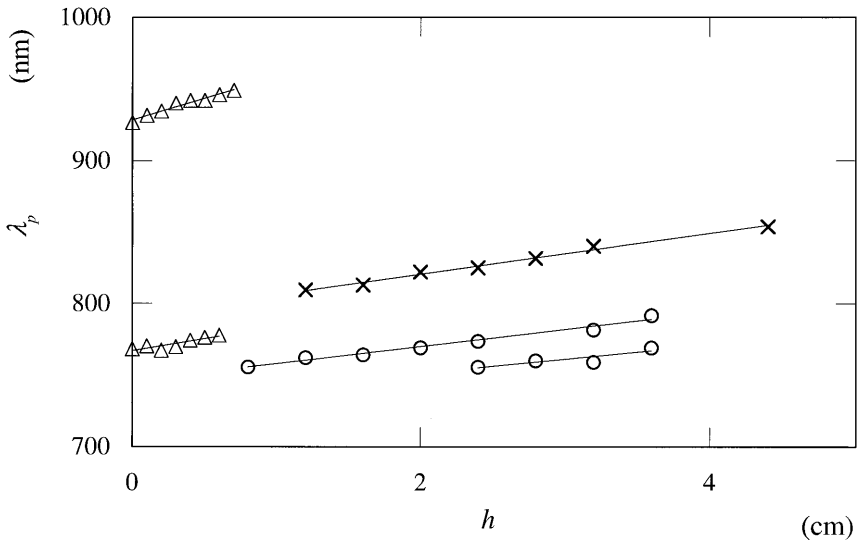

Fig. 4 Reflection peak wavelengths (λ_p) of the mixtures (1:1) as a function of height at 25 °C. O: CS82 and CS91 ($\phi_{CS82} = \phi_{CS91} = 0.01$); ×: CS82 and CS121 ($\phi_{CS82} = \phi_{CS121} = 0.01$); △: CS82 and CS161 ($\phi_{CS82} = \phi_{CS161} = 0.01$)

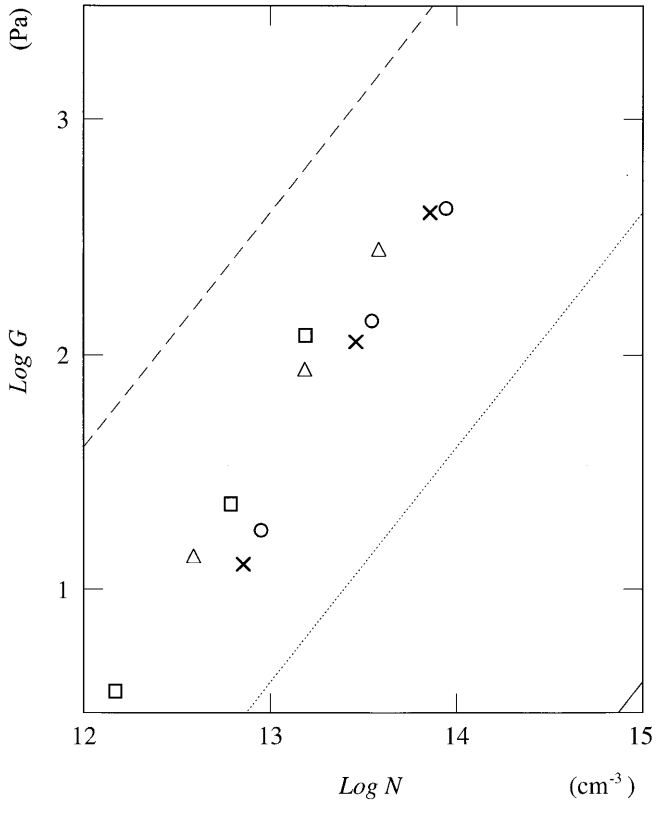

Fig. 5 Log G plotted as a function of log N. O: CS82, ×: CS91, △: CS121, □ : CS161. *Solid*, *dotted* and *broken lines* show the calculation at $g = 1$, 0.1, and 0.01, respectively

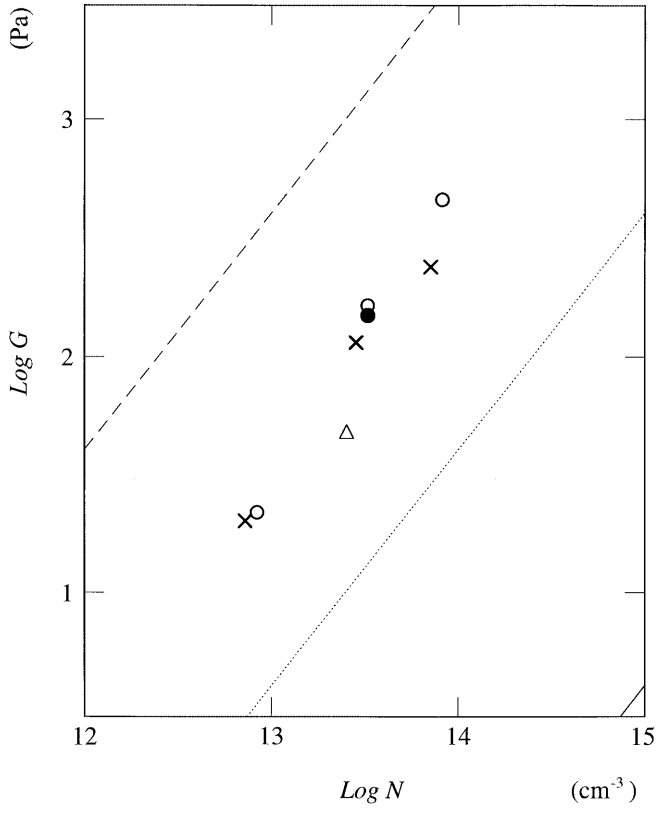

Fig. 6 Log G of the mixtures (2:1) as a function of log N. ○ (body-centered cubic, *bcc*), ● (face-centered cubic, *fcc*): CS82 and CS91, ×: CS82 and CS121, △: CS82 and CS161. *Solid*, *dotted* and *broken lines* show the calculation at $g = 1$, 0.1 and 0.01, respectively

three kinds of mixtures at various mixing ratios in volume fraction are shown in Figs. 6, 7 and 8. The order of magnitude of G is written in terms of the magnitude of the thermal fluctuation, δ, of a sphere as [5, 48]

$$G \sim f/l \sim (k_B T/\langle \delta^2 \rangle)/l \ , \tag{5}$$

where f is the force constant and δ is the thermal fluctuation of a sphere in the effective potential valley.

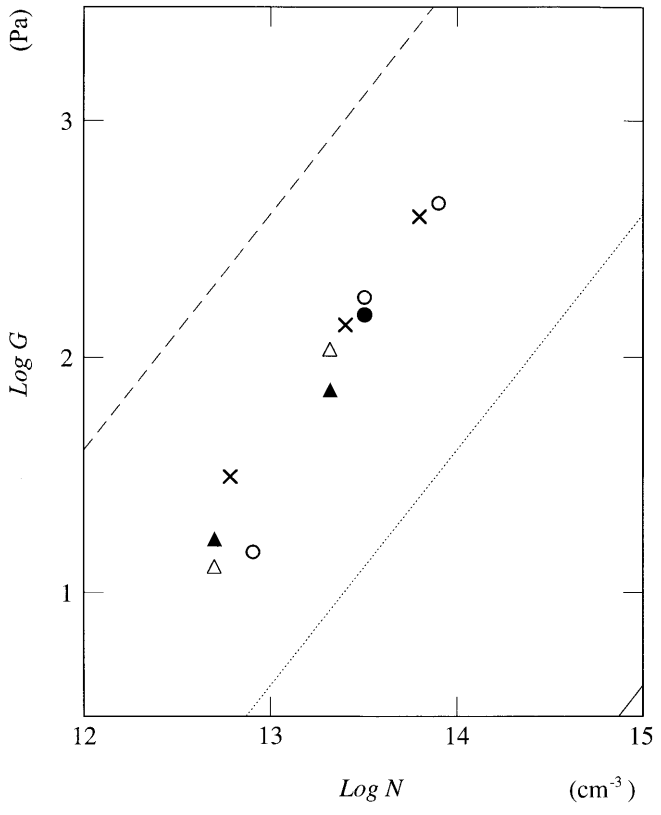

Fig. 7 Log G of the mixtures (1:1) as a function of log N. ○ (bcc), ● (fcc): CS82 and CS91, ×: CS82 and CS121, △: CS82 and CS161. *Solid*, *dotted* and *broken lines* show the calculation at $g = 1$, 0.1 and 0.01, respectively

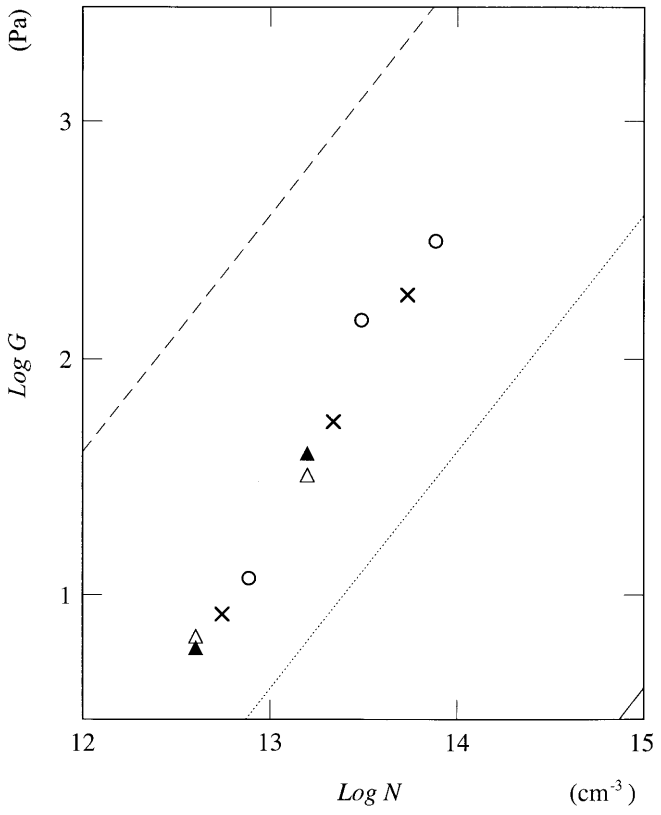

Fig. 8 Log G of the mixtures (1:2) as a function of log N. ○ : CS82 and CS91, ×: CS82 and CS121, △: CS82 and CS161. *Solid*, *dotted* and *broken lines* show the calculation at $g = 1$, 0.1 and 0.01, respectively

By introducing a nondimensional parameter, b, for $\langle\delta^2\rangle^{1/2}/l$, the modulus is obtained as a linear function of N:

$$G \sim Nk_{\mathrm{B}}T/b^2 \quad . \tag{6}$$

When $b = 1$ Eq. (6) gives the elastic modulus of an ideal gas having the same sphere concentration. Lindemann's law of crystal melting tells us that $b < 0.1$ holds for a stable crystal. The solid, dotted and broken lines in Figs. 5, 6, 7 and 8 represent the values of G when $b = 1$, 0.1 and 0.01, respectively. Clearly, all the G values in the figures are located between the dotted and broken lines. The b values estimated are also compiled in Tables 2, 3 and 4.

As is clear from Fig. 5, the rigidity of the colloidal crystals of the single component of spheres increased slightly as the size of the spheres increased at the same number density of spheres, which corresponds to the fact that the fluctuation parameter, b, decreased as the sphere size increased. Furthermore, the b values of the colloidal crystals decreased slightly as the sphere concentration increased. For example, the b values for CS82 decreased from 0.045 to 0.029 as is clear from Table 2. Clearly, stabler and more rigid crystals were formed as the sphere concentration and/or the sphere size increased. It should be noted here that generally speaking, the b values should be insensitive to the sphere sizes and/or sphere concentrations for the stable colloidal crystals including alloys. This interesting size effect observed in this work is explained by the fact that the volume fraction of the large spheres increases as their size increases even at the same number density of spheres and stabler crystals are formed from larger spheres. The main reason for the sphere concentration effect is ascribed to the fact that the degree of deionization with the resins for the diluted suspensions was not high enough during long measuring periods, 1–2 months.

The rigidities of colloidal alloys of CS82 mixtures with CS91, CS121 and CS161 with the same mixing ratio of 2:1 in volume fraction are shown in Fig. 6. Clearly, a sharp decrease in rigidity occurred when the size of the spheres mixed with CS82 spheres increased. These results mean that the colloidal alloys become less stable with the mixing of a small number of large pairing spheres, which have been reported in a previous work on the phase diagram of colloidal alloy [49]. Figures 7 and 8

show the log G versus log N plots when the volume fractions of the pairing spheres are 1:1 and 1:2, respectively. These figures also demonstrate that the rigidities of the colloidal alloys decrease, but only slightly, when the size of the pairing spheres with CS82 increases. However, we must omit one datum shown by the open circle at about 12.9 of log N in Fig. 7 in order to derive the previous conclusion.

Logarithms of the rigidities for the colloidal alloys of the mixtures with t various mixing ratios, 1:0, 2:1, 1:1, 1:2 and 0:1, were also plotted against log N, though the graphs showing these are omitted here. For the binary mixtures of CS82 and CS91, the rigidity increased as the ratio of the large spheres increased and then decreased passing a maximum at a 1:1 ratio. In other words, at the same total sphere number density the rigidity of the mixture was higher than that of the crystals of the single-component spheres. However, for mixtures of CS82 and CS121 and CS82 and CS161 these tendencies were not so clear, though the rigidities of 1:1 mixtures were always higher than the 1:0 mixtures.

In conclusion, sss-type alloy structures and $MgCu_2$-type superlattice structures were formed for the mixtures of CS82 and CS91 and CS82 and CS121, and CS82 and CS161, respectively. The rigidities of the colloidal alloys decreased when a comparatively small number of larger spheres (CS91, CS121 or CS161) were mixed with small spheres (CS82). The latter conclusion is consistent with the stability of the colloidal alloys clarified with the phase diagram experiments [49].

Acknowledgements M. Komatsu and M. Hirai of Catalysts & Chemicals Ind. Co. (Tokyo and Kitakyusyu) are greatly thanked for providing the silica samples. Akira Tsuchida of Gifu University is acknowledged for his valuable comments. The Ministry of Education, Science, Sports and Culture is thanked for Grants-in-Aid for Scientific Research on Priority Area (A) (11167241) and for Scientific Research (B) (11450367). T.O. thanks greatly the late Professor Emeritus Sei Hachisu for his continual encouragements and comments on our work on colloidal crystals.

References

1. Vanderhoff W, van de Hul HJ, Tausk RJM, Overbeek JThG (1970) In: Goldfinger G (ed) Clean surfaces: their preparation and characterization for interfacial studies. Dekker, New York, pp 15
2. Hiltner PA, Papir YS, Krieger IM (1971) J Phys Chem 75:1881
3. Kose A, Ozaki M, Takano K, Kobayashi Y, Hachisu S (1973) J Colloid Interface Sci 44:330
4. Williams R, Crandall RS, Wojtowicz PJ (1976) Phys Rev Lett 37:348
5. Mitaku S, Ohtsuki T, Kishimoto A, Okano K (1980) Biophys Chem 11:411
6. Lindsay HM, Chaikin PM (1982) J Chem Phys 76:3774
7. Pieranski P (1983) Contemp Phys 24:25
8. Ottewill RH (1985) Ber Bunsenges Phys Chem 89:517
9. Aastuen DJW, Clark NA, Cotter LK, Ackerson BJ (1986) Phys Rev Lett 57:1733
10. Pusey PN, van Megen W (1986) Nature 320:340
11. Okubo T (1988) Acc Chem Res 21:281
12. Russel WB, Saville DA, Schowalter WR (1989) Colloidal dispersions, Cambridge University Press, Cambridge
13. Sood AK (1991) Solid State Phys 45:2
14. Ackerson BJ, Clark NA (1981) Phys Rev Lett 46:123
15. Okubo T (1988) J Chem Soc Faraday Trans 1 84:1163
16. Monovoukas Y, Gast AP (1989) J Colloid Interface Sci 128:533
17. Aastuen DJW, Clark NA, Swindal JC, Muzny CD (1990) Phase Transitions 21:139
18. Okubo T (1991) J Chem Phys 95:3690
19. Okubo T (1992) Naturwissenschaften 79:317
20. Okubo T (1993) Prog Polym Sci 18: 481
21. Simon R, Palberg T, Leiderer P (1993) J Chem Phys 99:3030
22. Okubo T (1993) Colloid Polym Sci 271:190
23. Okubo T (1994) Langmuir 10:1695
24. Okubo T (1994) Langmuir 10:3529
25. Okubo T (1994) In: Schmitz KS (ed) Macro-ion characterization. From dilute solutions to complex fluids. ACS Symposium Series 548. American Chemical Society, Washington, DC, pp 364–380
26. Okubo T, Yoshimi H, Shimizu T, Ottewill RH (2000) Colloid Polym Sci 278:469
27. Russel WB (1990) Phase Transitions 21:127
28. Harkless CR, Singh MA, Nagler SE, Stephenson GB, Jordan-Sweet JL (1990) Phys Rev Lett 64:2285
29. Dhont JKG, Smits C, Lekkerkerker HNW (1992) J Colloid Interface Sci 152:386
30. Schatzel K, Ackerson BJ (1993) Phys Rev E 48:3766
31. Wurth N, Schwarz J, Culis F, Leidener P, Palberg T (1995) Phys Rev E 52:6415
32. van Megen W (1995) Transp Theory Stat Phys 24:1017
33. Hachisu S, Yoshimura S (1980) Nature 283:188
34. Yoshimura S, Hachisu S (1983) Prog Colloid Polym Sci 68:59
35. Okubo T (1990) J Chem Phys 93:8276
36. Okubo T (1986) J Chem Soc Faraday Trans 1 82:3163
37. Okubo T (1988) J Colloid Interface Sci 125:380
38. Okubo T (1987) J Chem Phys 86:2394
39. Dekker AJ (1957) Solid state physics. Prentice-Hall, New York, p 104
40. Yoshimura S, Hachisu S (1985) J Phys (Paris) 46:C3–115
41. Hachisu S, Kose A, Kobayashi Y (1987) J Colloid Interface Sci 55:499
42. Rosato AD, Standburg KJ, Prinz F, Swendsen RH (1987) Phys Rev Lett 58:1038
43. Jullien R, Meakin P, Pavlovitch A (1992) Phys Rev Lett 69:640
44. Knight JB, Jaeger HM, Nagel SR (1993) 70:3728
45. Zik O, Levine D, Lipson SG, Shtrikman S, Stavans J (1994) Phys Rev Lett 73:644
46. Vanel L, Rosato AD, Dave RN (1997) Phys Rev Lett 78:1255
47. Okubo T (1987) J Chem Soc 87:5528
48. Crandall RS, Williams R (1977) Science 198:293
49. Okubo T, Fujita H (1996) Colloid Polymer Sci 274:368